Nuclear Medicine and Biology 49 (2017) 57–64

Contents lists available at ScienceDirect

Nuclear Medicine and Biology

journal homepage: www.elsevier.com/locate/nucmedbio

Pancreas and liver uptake of new radiolabeled incretins (GLP-1 and Exendin-4) in models of diet-induced and diet-restricted obesity

Daniele Seo [a,*], Bluma Linkowski Faintuch [a], Erica Aparecida de Oliveira [b], Joel Faintuch [c]

[a] Radiopharmacy Center, Institute of Energy and Nuclear Research, Av. Prof. Lineu Prestes, 2242, São Paulo, 05508-000, Brazil
[b] School of Pharmaceutical Sciences, University of São Paulo, Av. Prof. Lineu Prestes, 580, Bloco 17, São Paulo, 05508-900, Brazil
[c] Department of Gastroenterology, Hospital das Clínicas, Av. Enéas C. Aguiar, 255, 9th Floor, Rm 9077, São Paulo, 05403-900, Brazil

ARTICLE INFO

Article history:
Received 16 November 2016
Received in revised form 2 February 2017
Accepted 15 March 2017
Available online xxxx

Keywords:
Technetium-99m
GLP-1 analogs
Diabetes
Obesity
Diagnostic imaging
Metabolic surgery

ABSTRACT

Introduction: Radiolabeled GLP-1 and its analog Exendin-4, have been employed in diabetes and insulinoma. No protocol in conventional Diet-Induced Obesity (DIO), and Diet-Restricted Obesity (DRO), has been identified. Aiming to assess pancreatic beta cell uptake in DIO and DRO, a protocol was designed.
Methods: GLP-1-βAla-HYNIC and HYNIC-βAla-Exendin-4 were labeled with technetium-99m. Four *Swiss* mouse models were adopted: Controls (C), Alloxan Diabetes Controls (ADC), DIO and DRO. Biodistribution and *ex-vivo* planar imaging were documented.
Results: Radiolabeling yield was in the range of 97% and both agents were hydrophilic. Fasting Blood Glucose (FBG) was 79.2 ± 8.2 mg/dl in C, 590.4 ± 23.3 mg/dl in ADC, 234.3 ± 66.7 mg/dl in DIO, and 96.6 ± 9.3 in DRO ($p = 0.010$). Biodistribution confirmed predominantly urinary excretion. DIO mice exhibited depressed uptake in liver and pancreas, for both radiomarkers, in the range of ADC. DRO only partially restored such values. ^{99m}Tc-HYNIC-βAla-Exendin-4 demonstrated better results than GLP-1-βAla-HYNIC-^{99m}Tc.
Conclusions: 1) Diet-induced obesity remarkably depressed beta cell uptake; 2) Restriction of obesity failed to normalize uptake, despite robust improvement of FBG; 3) HYNIC-βAla-Exendin-4 was the most useful marker; 4) Further studies are recommended in obesity and dieting, including bariatric surgery.

1. Introduction

Obesity has become a global health challenge and dieting for weight loss, including bariatric interventions, is now routine in many parts of the world. Derangements of glucose homeostasis are frequent in obesity, stimulating new diagnostic and follow-up protocols, for the monitoring of hepatic and pancreatic metabolic function. Changes in beta cell mass and function occur in both modalities of diabetes (type 1/T1D and 2/T2D), as well as in obesity and metabolic syndrome [1].

Glucagon-like-peptide-1 (GLP-1) impairment has been anticipated as the possible bridge between obesity and T2D. Improvement of GLP-1 has been associated with diabetes remission, after bariatric surgery [2,3,4].

GLP-1 receptor (GLP-1R) is has been adopted as a target, for noninvasive radiotracer monitoring of beta cell mass (BCM) in T2D, including obese diabetics, as well as insulinoma. Studies in these settings are increasing [5,6,7]. Indeed, BCM investigation with traditional immunological and functional tests, could render conflicting results, because of uncoupling between mass and function in many circumstances [8].

According to recent experimental evidence, GLP-1R imaging could simultaneously convey information about mass and function [9]. Improvement of both variables was analogously announced, after pharmacological administration of a GLP-1 agonist in a T1D model [10].

The major obstacle in the imaging of endogenous beta cell mass in the pancreas, is the low proportion of islet tissue, combined with its heterogenous distribution. It has been theorized that tracer uptake must be in excess of 1000 times, with regard to surrounding pancreatic tissues [11].

The incretin hormone GLP-1, secreted by enteroendocrine L cells, is an endogenous 30-amino-acid insulinotropic peptide that controls blood glucose levels *via* activation of GLP-1R on pancreatic beta-cells [12,13].

Exendin-4 is a 39 amino acid agonist of GLP-1, present in the saliva of the Gila monster (*Heloderma suspectum*). It has 53% homology with GLP-1, and a key difference in its C-terminus makes exendin-4 resistant to DPP-IV enzymatic degradation [14].

GLP-1 analogs have been radiolabeled with different radioisotopes, for diagnosis and therapy of benign and malignant insulinoma, as well for monitoring of T1D, T2D and islet cell transplantation [15].

Technetium-99m (^{99m}Tc) labeling has the advantage of optimal nuclear properties (half-life of 6 h and monochromatic 140 keV photons, along with favorable logistics, being transportable and easily available from ^{99}Mo/^{99m}Tc generators at low cost. Another advantage is biosafety, with 8 times less effective radiation compared to 68Ga, and 43 times less with regard to Indium-111 [15]. Such

* Corresponding author. Tel.: +55 11 97103 2797; fax: +55 11 3591 0033.
E-mail address: danyseo@uol.com.br (D. Seo).

http://dx.doi.org/10.1016/j.nucmedbio.2017.03.002
0969-8051/

radiolabeling has been performed using precursors including ^{99m}Tc-nitrido and ^{99m}Tc- tricarbonyl [16].

The most common approach for designing a target-specific ^{99m}Tc agent has been the attachment of a chelating group to the bioactive molecule, resulting in a combined ligand that can form a complex with ^{99m}Tc, in a reduced oxidation state. This bifunctional approach thus generates bifunctional chelating agents (BFCAs) [17].

The 2-Hydrazino-Nicotinic Acid (HYNIC) is a BFCA of great interest due to its high efficiency, fast radiolabeling and high radiolabeling yield [18,19].

The aim of this study was the evaluation of radiolabeled incretins (GLP-1 and Exendin-4 analog), in models of diet-induced obesity (DIO), and diet-restricted obesity (DRO). These models mimic typical populations in current obesity and bariatric practice, with shifts in glucose homeostasis ranging from insulin resistance to T2D. These include T2D remission and even cure, after sufficient weight loss [1]. Dynamics of BCM, which seem crucial for such outcome [2,3,4], are incompletely known. To the best of our knowledge, this is the first protocol targeting BCM by means of radiolabeled incretin analogs, in DIO and DRO.

2. Materials and methods

2.1. Materials

The conjugated incretins (HYNIC-β-Ala)-Exendin-4 [HGEGTFTSDLS KQMEEEAVRLFIEWLKNGGPSSGAPPPS] (MW = 4392.8) and GLP-1 [HAE GTFTSDVSSYLEGQAAKEFIAWLVKGR-K (HYNIC-β-Ala) NH2] (MW = 3632) were purchased from piChem Laboratory (Graz, Austria).

Tecnetium-99m (^{99m}Tc), in the form of Na^{99m}TcO4, was eluted from a ^{99}Mo/^{99m}Tc generator (Institute of Energy and Nuclear Research, IPEN/CNEN, São Paulo, Brazil), using 0.9% saline.

Silica gel strips (ITLC-SG, Gelman Science, Ann Arbor, MI, USA) were used for instant thin-layer chromatography. Reverse-phase high-performance liquid chromatography equipment (1260 Infinity HPLC system, Agilent Technologies, Santa Clara, CA, USA) was also performed using a Symmetry C-18 column (5.0 mm, 100 Å, 4.66250 mm, Waters, Milford, MA, USA). Radioactivity measurements were conducted using an automated, well-typed c-counter with NaI (Tl) crystal (Canberra, Meriden, CT, USA). All of the chemicals were reagent-grade (Sigma-Aldrich and Merck, São Paulo, Brazil). Accu Check Active glucose meter (Roche-Mannheim Germany) was used for blood glucose measure.

2.2. Animals and diets

Female *Swiss* albino mice (22–24 g) were used for the *in vivo* studies, always supplied by the Animal Facility of IPEN/CNEN, São Paulo, Brazil. C, ADC and DRO mice were fed normocaloric chow, *ad libitum* or in restricted amounts as appropriate (Nuvilab CR-1, Nuvital Nutrientes, Paraná, Brazil, containing 18% total lipids). A hyperlipidic, isonitrogenous diet was prepared for the DIO group, by addition of animal and vegetable fat and protein to the same chow, to a final concentration of 60% total lipids [9].

2.3. Methods

2.3.1. Ethical considerations

This protocol was approved by the Ethical Committee of the Institute of Energy and Nuclear Research, IPEN/CNEN, São Paulo, Brazil. All biological studies were carried out in accordance with the requirements of the Institutional Animal Welfare Committee, as well as the Brazilian College of Animal Experimentation.

2.3.2. Radiolabeling of conjugated peptides

Conjugated peptides were radiolabeled with ^{99m}Tc *via* a tricine transchelation reaction. In a sealed reaction vial containing 35 mg tricine dissolved in phosphate buffer 0.1 M, previously nitrogenated, was added 10 μL of a HYNIC-βAla-Exedin4 (227.64 μM) or 10 μL of GLP1-HYNIC-βAla (275.33 μM) solution plus 5 μL of 9 mM $SnCl_2.H_2O$ solution in 0.1 N HCl (nitrogen-purged) and 500 μL of Na^{99m}TcO$_4$ (740–1110 MBq). The mixture was heated for 20 min at 100 °C and cooled to room temperature; the pH of the final reaction was 7.

2.3.3. Radiochemical evaluation

Radiochemical analysis of the radiotracers was performed using instant thin-layer chromatography on silica gel strips (ITLC-SG), with a two solvent system, which consisted of methylethylketone (MEK) for $^{99m}TcO_4^-$ detection and a solution of 50% acetonitrile (ACN) for colloid detection ($^{99m}TcO_2$).

Each of the radiolabeled conjugates was also characterized by reverse-phase high-performance liquid chromatography analysis (RP-HPLC). All solvents used in the chromatographic analyses were HPLC-grade, and had been previously filtered through 0.22 mm membrane filters (Millipore, Milford, MA, USA).

The HPLC solvents consisted of H_2O containing 0.1% trifluoroacetic acid (Solvent A), and acetonitrile containing 0.1% trifluoroacetic acid (Solvent B), with a flow rate of 1 ml/min. The HPLC gradient system began with a solvent composition of 95% A and 5% B, and followed a linear gradient of 30% A: 70% B, from 0 to 25 min, and 5% A: 95% B from 25 to 30 min.

2.3.4. Partition coefficient of the radiotracers

Partition coefficient of the radiotracers was evaluated in octanol/water (1:1), as previously described [20]. A sample (100 μL) was dissolved in the mixture, and then vigorously stirred and centrifuged at 5000 ×*g* for 3 min. Aliquots (in triplicate) from both phases (n-octanol and water) were collected, and their radioactivity was measured using a gamma counter. The partition coefficient was expressed as log P = log (activity in octanol phase/activity in water phase).

2.3.5. Design of biological studies

The *in vivo* studies were performed in female *Swiss* mice (22–24 g). Animals were housed individually in cages, and were provided water *ad libitum*, and diets according to the protocol. For all animal models, biodistribution of the radiotracers was evaluated, with *ex-vivo* quantification by scintigraphy images. Also histological analysis of the liver and pancreas at the end of the investigation was provided. Five animals per experimental group (ADC, DIO, DRO) were utilized for each radiotracer, for a subtotal of 30 animals. The control group was studied at 4 different time points, for each radiotracer. With 5 animals/group, the subtotal was 40 animals. Five additional animals for each group were employed during histological analysis (20 more). The grand total was 90 mice.

2.3.6. Animal groups

- Control animals (C)

This group was maintained on normal chow *ad libitum* during 60 days, with no intervention.

- Alloxan Diabetes Controls (ADC)

These mice were handled similarly to group C until the 57th day. Then alloxan monohydrate (Sigma-Aldrich, Sao Paulo, Brazil), dissolved in 0.01 M citrate buffer pH 4.5 was intraperitoneally injected, after a 12-h fast, at a single dose of 150 mg/kg body weight. Only mice with FBG values >300 mg/dl on the next day, were considered for this study [10].

- Diet-Induced Obesity

A hyperlipidic diet (60% fat) was employed during 30 days [9], after 30 days with normal chow. Vegetable and animal fat and protein were added to the standard feed (18% fat), in order to achieve the desired concentration. The energy value of this mixture corresponded to approximately 5600 kcal/kg, *vs.* 3860 kcal/kg for regular chow.

- Diet-Restricted Obesity

Obesity was triggered as in the former group, with the hyperlipidic diet. In the subsequent 30 days, normal chow was restarted, however

in the diminished proportion of 50 kcal/week only [21]. The aim was to achieve a 30% decrease in body mass, similar to what is accomplished after bariatric and metabolic surgery [2,3,4].

2.3.7. Metabolic variables

Body weight was registered once a week, and FBG was measured at baseline, and after 60 days. Only ADC animals were additionally tested for FBG, as alluded to.

2.3.8. Biodistribution study and imaging evaluation

The incretin 50 μL (37 MBq/75 pmol) was injected into the tail vein, and sacrifice was conducted after different times (10, 30, 60 and 120 min), for control animals. Biodistribution in ADC, DIO, and DRO animals was done at one time point only, 60 min, based on the best pharmacokinetics in C.

Organ and tissue samples were excised, weighted and radioactivity measured in a gamma counter (Packard Cobra Quantum 5002, GMI, Ramsey, MN, USA), using the injected dose as standard for calculation. Results were expressed in percentage of injected dose per gram (%ID/g).

The uptake of the radiotracer in liver, pancreas, heart and intestine (small and large) was evaluated in *ex vivo* images, held in a gamma camera with a LEHR collimator of Mediso Imaging System, Budapest, Hungary. Images were acquired using a 256 × 256 × 16 matrix size, with a 20% energy window set at 140 keV, for a period of 180 s. The region of interest (ROI) of the organs was quantified, considering the injected dose as standard.

2.3.9. Histological screening

Hematoxylin/eosin slides of the pancreas and liver were processed in the Department of Stomatology, Dental School, University of São Paulo. The objectives were investigation of fatty liver disease, in both DIO and DRO, as well as confirmation of alloxan effects on liver and pancreas, in ADC. Hormone-specific histochemical analysis and *in-situ* hybridization could not be provided, in the conditions of this study. Images were interpreted by expert pathologists at the Veterinary Center of Pathological Anatomy., University of São Paulo.

2.3.10. Statistical analysis

Findings are presented as mean ± SD. Changes of single groups were compared by Student's "t" test. Analysis of variance (ANOVA) and post-hoc Tukey test were adopted for group comparisons. Pearson regression analysis was employed for correlation between GLP1 and Exendin 4 results, *vs.* body weight and FBG in the various groups. In all circumstances, $p < 0.05$ was considered significant. The Bioestat program version 5.0 (Bioestat.software.informer.com) was employed.

Table 1
Metabolic findings in the four groups.

Group	Final body weight (g)	Final FBG
C	23.4 ± 0.5	79.2 ± 8.2
ADC	23.0 ± 0.6	590.4 ± 23.3
DIO	44.7 ± 4.6	234.3 ± 66.7
DRO	31.5 ± 4.3	96.6 ± 9.3

C (Control), DIO (Diet-Induced Obesity), ADC (Alloxan Diabetes Controls) DRO (Diet-Restricted Obesity), FBG: Fasting Blood Glucose, mg/dL.

3. Results

3.1. Radiolabeling of conjugated peptides

Both conjugates were radiolabeled using the same protocol. The radiochemical purities of ^{99m}Tc-HYNIC-β-Ala-Exedin4 and GLP1-β-Ala-HYNIC-Tc^{99m} were 97.1 ± 1.6% and 97.1 ± 0.7%, the corresponding retention times by HPLC were 18.463 min and 18.48 min, (Fig. 1) and the specific activity was 486.8 MBq/nmol, and 402.2 MBq/nmol, respectively for each radiotracer.

The lipophilicity of the radiotracers was determined according to their proportional distribution between octanol and water. Both results are in the range of hydrophilicity. The *log P* value was −0.89 ± 0.02 for the GLP-1 tracer and −1.33 ± 0.09 for the Exendin-4 tracer, showing a higher hydrophilicity for the latest, with significant difference ($p < 0.01$).

3.2. Animal models

Body weight and FBG at the end of the experimental period (60 days), in the four groups, are displayed in Table 1.

Fig. 2 depicts the FBG profile of DRO, which resembles what is observed in intensive pharmacological treatment of T2D, as well as in bariatric/metabolic procedures.

3.3. Biodistribution study and imaging evaluation

Biodistribution in controls at different time points (Table 2), revealed more remarkable lung uptake for Exendin-4 than for GLP-1. Rapid blood clearance (approximately 80% decrease) occurred after 60 min, with a similar pattern for both products.

Renal uptake predominated for both radiotracers, indicating the urinary system as the major excretory pathway, yet hepatobiliary excretion was also detected.

High uptake was observed in the pancreas, 10 min after administration of the radiotracers. ^{99m}Tc-HYNIC-Exendin-4 was more prominent

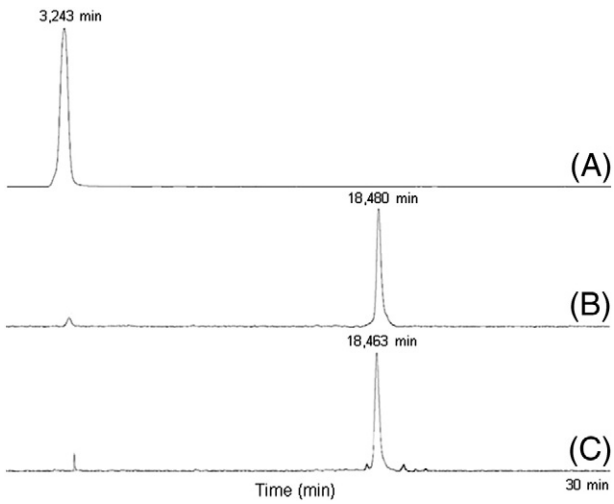

Fig. 1. Reverse-phase HPLC profile: (A) $Na^{99m}TcO_4$; (B) GLP1-β-Ala-HYNIC-^{99m}Tc; (C) ^{99m}Tc-HYNIC-β-Ala-Exendin4.

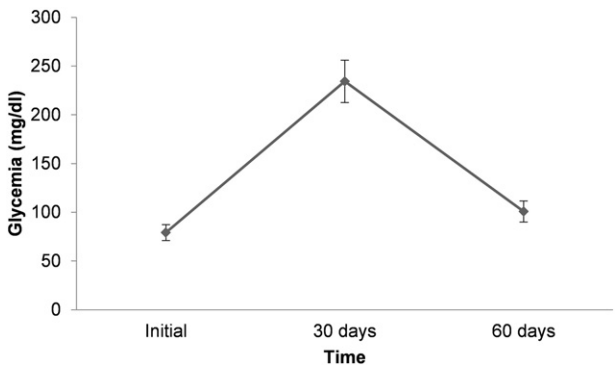

Fig. 2. Fasting blood glucose in diet-restricted obesity.

Table 2
Biodistribution of the ^{99m}Tc conjugates in control *Swiss* mice.

Tissue	Time							
	10 min		30 min		60 min		120 min	
	GLP-1*	Exendin-4**	GLP-1	Exendin-4	GLP-1	Exendin-4	GLP-1	Exendin-4
Blood	13.25 ± 1.53	9.71 ± 2.42	4.78 ± 0.37	5.95 ± 1.53	1.22 ± 0.13	1.02 ± 0.41	0.51 ± 0.07	0.49 ± 0.10
Heart	3.95 ± 0.67	3.74 ± 0.50	1.57 ± 0.34	3.76 ± 0.30	0.81 ± 0.11	0.96 ± 0.17	0.42 ± 0.06	0.37 ± 0.21
Lung	10.49 ± 0.97	19.84 ± 0.42	3.36 ± 0.61	9.78 ± 0.98	2.09 ± 0.25	5.50 ± 0.71	1.38 ± 0.33	1.54 ± 0.10
Kidney	76.90 ± 3.43	64.06 ± 4.30	53.74 ± 2.86	50.78 ± 3.91	61.69 ± 2.20	47.72 ± 4.83	51.27 ± 1.74	35.63 ± 0.96
Spleen	5.23 ± 0.09	6.62 ± 0.15	2.53 ± 0.42	4.35 ± 0.40	1.35 ± 0.18	1.40 ± 0.50	1.18 ± 0.06	1.43 ± 0.43
Stomach	2.51 ± 0.10	2.97 ± 0.21	1.52 ± 0.16	2.89 ± 0.53	1.55 ± 0.16	2.85 ± 0.43	1.63 ± 0.03	1.76 ± 0.23
Pancreas	6.46 ± 0.35	8.66 ± 0.60	2.24 ± 0.28	4.76 ± 0.51	1.10 ± 0.14	1.77 ± 0.33	0.52 ± 0.04	0.50 ± 0.22
Liver	5.52 ± 0.65	5.16 ± 0.29	3.22 ± 0.52	3.33 ± 0.81	2.06 ± 0.13	1.61 ± 0.44	1.60 ± 0.38	1.03 ± 0.13
Large I.	7.19 ± 1.33	5.98 ± 1.09	2.84 ± 0.30	3.62 ± 0.79	1.24 ± 0.35	1.51 ± 0.26	0.50 ± 0.05	0.72 ± 0.48
Small I.	4.82 ± 0.66	6.14 ± 1.15	2.53 ± 0.38	4.72 ± 1.11	1.03 ± 0.10	2.53 ± 0.48	0.89 ± 0.16	1.35 ± 0.14
Muscle	2.58 ± 0.20	2.12 ± 0.56	2.55 ± 0.67	1.87 ± 0.71	0.40 ± 0.10	0.44 ± 0.10	0.30 ± 0.06	0.15 ± 0.01
Bone	4.99 ± 0.27	4.99 ± 0.60	2.40 ± 0.27	2.52 ± 0.64	1.05 ± 0.27	1.05 ± 0.09	0.49 ± 0.08	0.85 ± 0.03

Abbreviations: I. Intestine:
(*)GLP-1-β-Ala-HYNIC-^{99m}Tc; (**)^{99m}Tc-HYNIC-β-Ala-Exendin-4.
Data are expressed as the mean ± SD (n = 5). The radioactivity in the stomach and intestine was evaluated after thoroughly removing the luminal contents.

($p < 0.01$) than GLP1-β-Ala-HYNIC-Tc^{99m}, at 30 and 60 min post-injection.

Tables 3 and 4 display the biodistribution results for both radiotracers in all four groups, 60 min after administration. Similar profiles can be observed for both radiotracers.

No group achieved liver and pancreas uptakes equal to controls. ADC and DIO performed worst in this regard. A tendency toward recovery could be unveiled in DRO, however clearly below full restoration. ^{99m}Tc-HYNIC-β-Ala-Exendin-4 performed better than GLP-1-β-Ala-HYNIC-^{99m}Tc, with more favorable pancreas/blood ratio.

Ex-vivo gamma camera imaging of liver, pancreas, large intestine, small intestine and heart, in the same groups (Figs. 3 and 4), confirmed that highest uptake was in the liver. Region of interest (ROI) results fluctuated from 0.47 to 1.12% for this viscus, followed by small intestine (0.05–0.53%). Values in the pancreas were always low for the three intervention groups, compared to control animals.

Correlation between pancreatic uptake in the various groups, and FBG, was significant for GLP-1 only ($P = 0.047$). None of the two radiotracers correlated with body weight in the same groups.

3.4. Histological screening

The liver and pancreas were histologically screened for fatty liver disease, as well as pancreatic islet size and morphology.

Fatty liver disease was not confirmed in DIO or DRO. Occasional steatosis and inflammatory infiltrate in the central venular zone were registered in ADC (Fig. 5).

Diameter of islet cells was mildly increased in the pancreas of DIO and DRO, consistent with beta-cell stress and hyperplasia [22] (Fig. 6). In ADC animals, disruption of the islets of Langerhans, along with inflammatory infiltrate, occurred as expected (Fig. 6).

4. Discussion

Beta cells are believed to play a crucial role, in two of the most important chronic nontransmissible diseases, namely obesity and diabetes [2–4,23]. Nevertheless, technical and anatomical barriers have notably retarded the implementation of diagnostic techniques, for the monitoring of BCM in the islets of Langerhans. Metabolic studies, which are the most widely employed in clinical practice, may not accurately reflect beta-cell damage, except in the extremes of intact performance *versus* advanced impairment [8].

The European Commission recently launched the Innovative Medicines Initiative in Diabetes, including among its goals, noninvasive means to measure BCM *in vivo*. It concluded that ultrasonography and CT lack specificity, whereas MRI and fluorescent methods also suffer from serious bottlenecks. Perspectives for PET are more optimistic, however that would still require a new generation of radiotracers, including highly specific beta-cell ligands. Multimodal approaches, possibly combining fluorescent, MRI and PET-active moieties, could be adopted in the meantime, even though these are expensive and cumbersome [24].

GLP-1R incretin-based targeting molecules, particularly Exendin-4 due to its unequaled specificity, seem well positioned as a convenient

Table 3
Biodistribution of GLP1-β-Ala-HYNIC-^{99m}Tc (%ID/g) in C, ADC, DIO and DRO *Swiss* mice (n = 5).

Radiotracer	GLP-1-βAla-HYNIC-^{99m}Tc				
Time	60 min				
	C	DIO	ADC	DRO	P
Blood	1.22 ± 0.13	1.05 ± 0.05	0.56 ± 0.01	0.99 ± 0.14	0.032
Heart	0.81 ± 0.11	0.35 ± 0.03	0.30 ± 0.04	0.35 ± 0.03	0.003
Lung	2.09 ± 0.25	1.42 ± 0.37	0.81 ± 0.13	1.27 ± 0.21	0.014
Kidney	61.69 ± 2.20	76.89 ± 4.99	83.63 ± 3.60	80.83 ± 4.70	0.398
Spleen	1.35 ± 0.18	0.72 ± 0.06	0.84 ± 0.11	0.68 ± 0.10	0.030
Stomach	1.55 ± 0.16	1.97 ± 0.23	1.47 ± 0.38	1.78 ± 0.89	0.028
Pancreas	1.10 ± 0.14	0.95 ± 0.13	0.81 ± 0.10	1.01 ± 0.12	0.048
Liver	2.06 ± 0.13	1.09 ± 0.15	1.33 ± 0.23	1.36 ± 0.32	0.019
Large Intestine	1.24 ± 0.35	1.06 ± 0.08	0.70 ± 0.04	0.64 ± 0.07	0.014
Small Intestine	1.03 ± 0.10	1.15 ± 0.30	0.93 ± 0.09	0.86 ± 0.09	0.266
Muscle	0.40 ± 0.10	0.25 ± 0.04	0.24 ± 0.04	0.27 ± 0.02	0.111
Bone	1.05 ± 0.27	0.41 ± 0.08	0.52 ± 0.11	0.17 ± 0.05	0.036

Data are expressed as the mean ± SD (n = 5). The radioactivity in the stomach and intestine was evaluated after thoroughly removing the luminal contents. C (control), DIO (diet-induced obesity), ADC (alloxan diabetes controls) DRO (diet-restricted obesity).

Table 4
Biodistribution of ^{99m}Tc-HYNIC-β-Ala-Exendin-4 (%ID/g) in C, ADC, DIO and DRO *Swiss* mice (n = 5).

Radiotracer	^{99m}Tc-HYNIC-βAla-Exendin4				
Time	60 min				
	C	DIO	ADC	DRO	P
Blood	1.02 ± 0.41	0.62 ± 0.10	0.36 ± 0.06	0.54 ± 0.06	0.024
Heart	0.96 ± 0.17	0.40 ± 0.06	0.37 ± 0.11	0.28 ± 0.07	0.011
Lung	5.50 ± 0.71	5.13 ± 0.86	2.02 ± 0.11	3.68 ± 0.17	0.009
Kidney	47.72 ± 4.83	66.19 ± 1.98	37.06 ± 5.46	68.58 ± 6.66	0.073
Spleen	1.40 ± 0.50	0.49 ± 0.03	0.25 ± 0.08	0.56 ± 0.11	0.016
Stomach	2.85 ± 0.43	2.15 ± 0.37	1.94 ± 0.33	2.28 ± 0.18	0.030
Pancreas	1.77 ± 0.33	1.16 ± 0.05	0.90 ± 0.06	1.29 ± 0.14	0.035
Liver	1.61 ± 0.44	0.56 ± 0.07	0.65 ± 0.07	0.76 ± 0.09	0.006
Large Intestine	1.51 ± 0.26	1.29 ± 0.07	0.91 ± 0.07	1.01 ± 0.23	0.027
Small Intestine	2.53 ± 0.48	1.40 ± 0.10	0.48 ± 0.09	1.15 ± 0.19	0.014
Muscle	0.44 ± 0.10	0.33 ± 0.04	0.15 ± 0.01	0.17 ± 0.04	0.152
Bone	1.05 ± 0.09	0.44 ± 0.10	0.36 ± 0.05	0.43 ± 0.08	0.031

Data are expressed as mean ± SD (n = 5). The radioactivity in the stomach and intestine was evaluated after thoroughly removing the luminal contents. C (control), DIO (diet-induced obesity), ADC (alloxan diabetes controls) DRO (diet-restricted obesity).

marker [5–7,9]. It resists the exo- and endo-peptidases which rapidly cleave GLP- 1, and efficiently binds to GLP-1R. Much of its superiority concerning GLP-1, is related to the central helical region, and the contrasting sequences of Leu10-Gly30 in Exendin- 4, *vs.* Val16-Arg36 in GLP-1 [25].

The binding site of the chelator, in the case of ^{99m}Tc radiomarkers, can influence pharmacokinetics, and binding affinity as well. In several protocols, the chelator (mainly DOTA) is attached to a Lys^{40}. In the current investigation, HYNIC was attached to the N terminal of Exendin-4, due the functional importance of the PSSGAPPPS sequence, for the N-terminal affinity to the target receptor [26].

In a pilot study, radiolabeling was done using EDDA-tricine coligands exchange (data not shown), resulting in a low profile. Using only tricine as coligand to complete the coordination sphere of the technetium (V) core, a higher yield was achieved, with good radiochemical stability.

High kidney uptake was probably a consequence of the utilization of HYNIC, and the beta alanine amino acid as a spacer. Yet, some hepatobiliary excretion also emerged. Even though ^{99m}Tc-HYNIC-βAla-Exendin-4 is more hydrophilic, its renal excretion was exceeded by GLP-1-βAla-HYNIC-^{99m}Tc. Probably the short biological half-life of GLP-1, due to rapid hydrolysis, was responsible for faster clearance.

GIP could be an interesting molecule to test in the current model. However GIP is as susceptible as GLP-1, to degradation by the enzyme dipeptidyl peptidase-4 (DPP-4). DPP-4-resistant GIP agonists are being developed, however they are still far from routine use.

The adult pancreas houses roughly one million islets, in which beta cells represent nearly 75% [23]. Even though genetically shaped to sense and respond to FBG shifts, chronic hyperglycemia is an aggression to such cells, triggering apoptosis and disrupted cell autophagy [23,27,28].

There are reasons to believe that the onset of BCM compromise, is at least one decade before diabetes materializes [29]; indeed in prediabetes, insulin response to diet-released GLP-1 is already impaired, even though FBG changes in such circumstances are mild, and easily reversed [23,28].

Beta cells, or at least precursor or related cells, are dynamic and try to restore glucose homeostasis. In obesity, moderate increase in BCM is consistently reported [22]. Of course in T2D pancreatic exhaustion eventually ensues, with collapse of the beta cell population.

These hypotheses were in agreement with histological findings. Islet cells suggestive of hyperplasia were unveiled in the slides, of both DIO and DRO mice, consistent with deranged FBG in such populations. The fact that FBG failed to normalize, doesn't rule out a corrective effort of the pancreas. Beta cell dysfunction, unable to keep up with high insulin demands, seems the most probable explanation, analogously to what is postulated in the pathophysiology of type 2 diabetes [8].

Nor does compensatory hyperplasia conflict with the notably lower radiotracer uptake, in these two populations. As alluded to, pancreatic islets are a dynamic environment, in which different tendencies may co-exist, such as apoptosis, cell autophagy, and hyperplasia. Despite some positive histological evidence, dysfunction was certainly overwhelming in DIO and DRO mice, thus BCM decrease and hyperglycemia could not be avoided.

It is generally accepted that GLP-1 receptor is expressed in the pancreatic islet cells, the intestine, lungs and kidneys; however recent investigations include the liver as well [30]. Moreover, it plays protean roles in metabolism, immune response, critical illness, and even hyperlipidic diet effects. For instance, links between GLP-1R mRNA and thymus, spleen, bone marrow, as well as assorted immune cells, included those in the intestinal mucosa, have been identified [31]. Endotoxemia and critical illness activate GLP-1R receptors [32]. Our groups included two modalities of obesity and also type-1 diabetes, all of them believed to involve a certain degree of systemic inflammation. These may partly explain the mild fluctuations in radiotracer uptake, observed among different organs and models.

A depressed profile of incretin response was prominent in the liver, as occurred as well in the intestine and other sites.

There is reliable evidence that GLP-1 receptor is expressed in the liver. Within the context of nonalcoholic fatty liver disease (NAFLD),

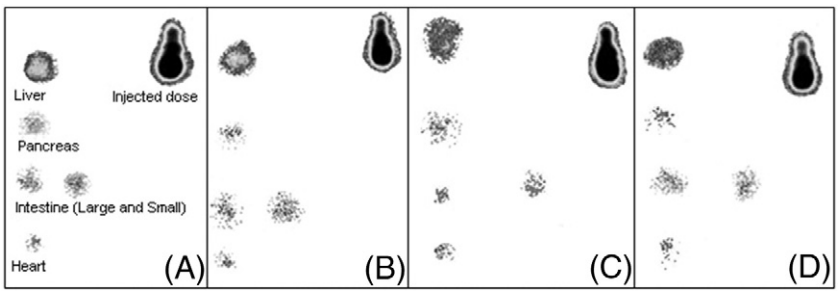

Fig. 3. *Ex-vivo* images in controls (A), diet-induced obesity (B), alloxan diabetes controls (C), and diet-restricted obesity (D), 60 min post-injection of GLP-1-β-Ala-HYNIC-^{99m}Tc.

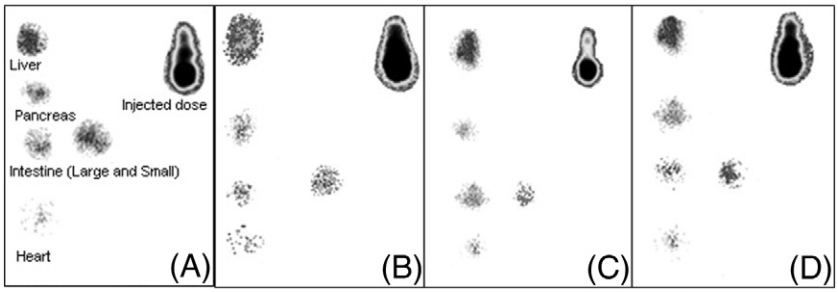

Fig. 4. *Ex-vivo* images in controls (A), diet-induced obesity (B), alloxan diabetes controls (C), and diet-restricted obesity (D), 60 min post-injection of ^{99m}Tc-HYNIC-β-Ala-Exendin-4.

there are meta-analyses with hundreds of patients, confirming the role of GLP-1R in the liver [33,34].

Despite such implications with NAFLD, no significant lipid infiltration was documented in the hepatocytes of DIO and DRO groups, probably because of the relatively short duration of obesity.

Only FBG in the various groups correlated with GLP-1 results, no significance being achieved for body weight or for FBG in the Exendin-4 protocol. This lack of correlation was expected, as beta-cell failure without actual reduction in beta cell mass, has been suspected by others in DIO [35].

In a recent article using Gallium-labeled Exendin 4 in pigs, hypoglycemia and severe tachycardia were noticed [36]. As a consequence the authors suggested cutoff points. For glucose abnormalities the value was ≥ 0.14 μg/kg, and for cardiovascular side effects, including possible heart arrest ≥ 2.8 μg/kg.

Biodistribution equivalence for different species has been already calculated, in an experience with a somewhat different gallium-labeled Exendin-4 molecule: 0.017 ± 0.004 (rats), 0.014 ± 0.004 (pigs), 0.017 ± 0.004 (NHP), and 0.016 (human) mSv/MBq. Albeit species fluctuations occurred, the order of magnitude was the same in all circumstances [37].

The aforementioned safety limits are often exceeded, as was the case in the present protocol, as well as many others. No additional report of glucose homeostasis or cardiac function shifts could be identified in the literature with Exendin-4 labeled by different tracers, in any species.

One doesn't doubt that the reported complications occurred, and deserve further studies. However an idiosyncratic response, not a regular feature of the radiomolecules, should be suspected. In our current experience as well as in other recent protocols, heart arrest or convulsions never occurred, even though over a hundred animals were injected.

In synthesis, obesity was associated with serious reduction of BCM response in the pancreas and liver, as highlighted by the GLP-1 and Exendin-4 radiomarkers. The decrease was practically identical to alloxan diabetes, which is a very severe modality of beta cell dysfunction. Therapeutic weight loss, in the range commonly observed after bariatric and metabolic surgery, even though substantially beneficial for body weight and FBG, was followed by less encouraging rehabilitation of BCM.

This is the first study which, to our knowledge, describes the incretin radiotracer profile of BCM, in diet-induced and diet-reversed obesity. The weaknesses of the protocol include the relatively short duration of the obesity period, and the single time point assessment. Lack of histochemical demonstration of GLP-1 receptor binding is also a weak point.

Diet induced obesity in rodents exists for nearly 70 years [38], and review articles are available [39]. Partial or total reversal of DIO is more recent; however it is no novelty anymore. The hyperlipidic (60% fat) and the low fat regimens (18–20% lipids), as here adopted, are probably the most popular. Induction may last from one to ten months, and reversal may be conducted at different time points as well.

The endocrinological literature is typically concerned with body composition, glucose homeostasis, hormones, and inflammation markers. For the purpose of tracking beta cell shifts, such variables

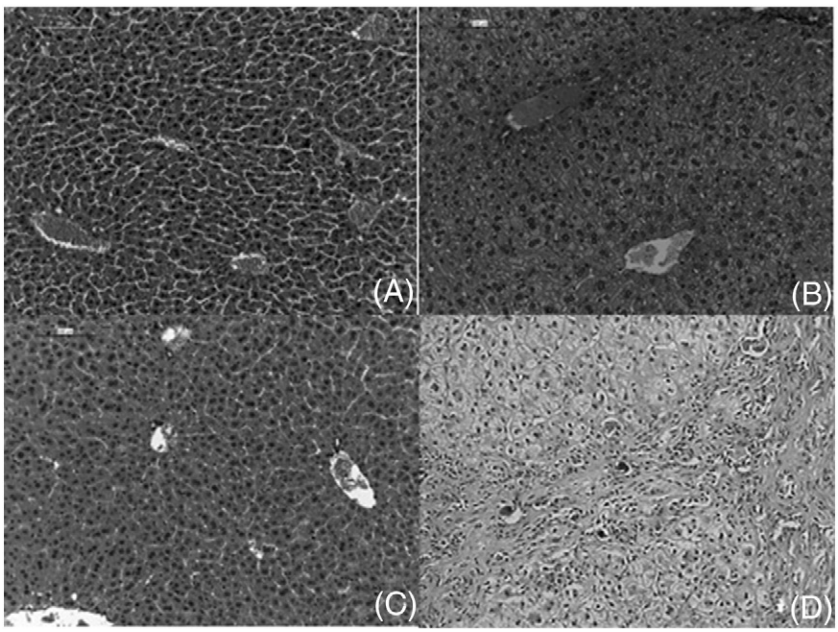

Fig. 5. Histological sections of liver; (A) controls; (B) diet-induced obesity; (C) alloxan diabetes controls; (D) diet-restricted obesity. Hematoxylin–eosin staining, 20× magnification.

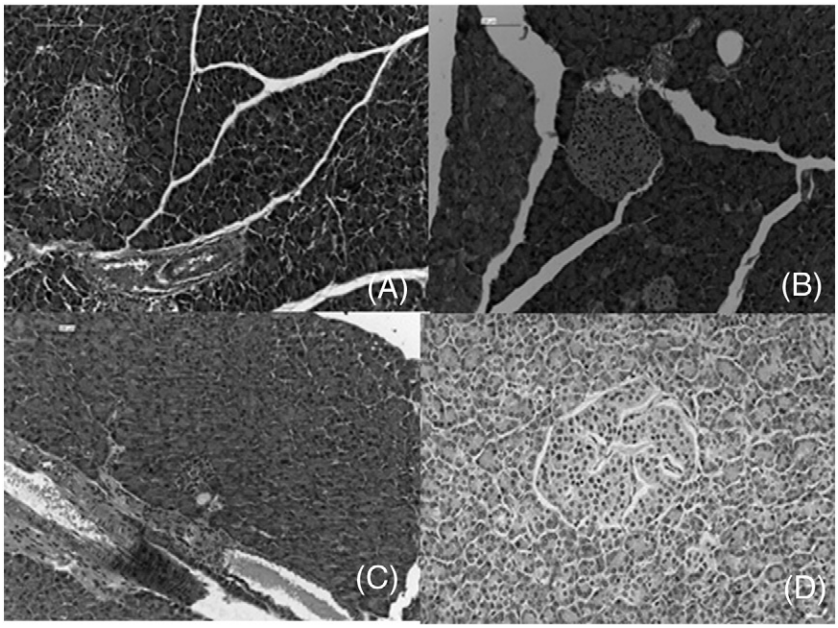

Fig. 6. Histological sections of pancreas; (A) controls; (B) diet-induced obesity; (C) alloxan diabetes controls; (D) diet-restricted obesity. Hematoxylin- eosin staining, 20× magnification.

would not be irrelevant. Nevertheless, the central end-points should be radiotracer monitoring of GLP-1R, with histochemical and molecular confirmation of beta cell abundance and insulin expression.

5. Conclusions

1) Diet-induced obesity remarkably depressed beta cell uptake; 2) Restriction of obesity failed to normalize uptake, despite robust improvement of FBG; 3) HYNIC-βAla-Exendin-4 was the most useful marker for beta cell mass in both diet-induced and diet-restricted obesity; 4) Further studies are recommended in obesity and dieting, including bariatric surgery.

Conflict of interest

None.

Acknowledgment

The authors are indebted to the National Commission for Nuclear Energy (CNEN, São Paulo, Brazil) and National Counsel of Technological and Scientific Development (CNPq, Brasilia, Brazil) for scientific grants. We are grateful to Natanael Gomes da Silva for their technical support during the animal experiments and imaging procedures. We also thank Maria Neide Ferreira Mascarenhas for her cooperation regarding the animal facilities.

References

[1] Kashyap SR, Louis ES, Kirwan JP. Weight loss as a cure for type 2 diabetes? Fact or fantasy. Expert Rev Endocrinol Metab 2011;6:557–61.
[2] Amouyal C, Andreelli F. Increasing GLP-1 circulating levels by bariatric surgery or by GLP-1 receptor agonists therapy: why are the clinical consequences so different? J Diabetes Res 2016;2016:1–10.
[3] Salehi M, Gastaldelli A, D'Alessio DA. Altered islet function and insulin clearance cause hyperinsulinemia in gastric bypass patients with symptoms of postprandial hypoglycemia. J Clin Endocrinol Metab 2014;99:2008–17.
[4] Sista F, Abruzzese V, Clementi M, Carandina S, Amicucci G. Effect of resected gastric volume on ghrelin and GLP-1 plasma levels: a prospective study. J Gastrointest Surg 2016;20:1931–41.
[5] Mi B, Xu Y, Pan D, Wang L, Yang R, Yu C, et al. Non-invasive glucagon-like peptide-1 receptor imaging in pancreas with (18)F-al labeled Cys(39)-exendin-4. Biochem Biophys Res Commun 2016;471:47–51.
[6] Bandara N, Zheleznyak A, Cherukuri K, Griffith DA, Limberakis C, Tess DA, et al. Evaluation of cu-64 and Ga-68 radiolabeled glucagon-like peptide-1 receptor agonists as PET tracers for pancreatic β cell imaging. Mol Imaging Biol 2016;18:90–8.
[7] Wu Z, Liu S, Nair I, Omori K, Scott S, Todorov I, et al. ^{64}Cu labeled sarcophagine exendin-4 for microPET imaging of glucagon like peptide-1 receptor expression. Theranostics 2014;4:770–7.
[8] Meier JJ, Bonadonna RC. Role of reduced β-cell mass versus impaired β-cell function in the pathogenesis of type 2 diabetes. Diabetes Care 2013;36:S113–9.
[9] Lehtonen J, Schäffer L, Rasch MG, Hecksher-Sørensen J, Ahnfelt-Rønne J. Beta cell specific probing with fluorescent exendin-4 is progressively reduced in type 2 diabetic mouse models. Islets 2015;7 e1137415-1 e1137415-10.
[10] Tamura K, Minami K, Kudo M, Iemoto K, Takahashi H, Seino S. Liraglutide improves pancreatic beta cell mass and function in alloxan-induced diabetic mice. PLoS One 2015;10:1–15.
[11] Eriksson O, Alavi A. Imaing the islet graft by positron emission tomography. Eur J Nucl Med Mol Imaging 2012;39:533–42.
[12] Gallwitz B. Glucagon-like peptide-1 analogues for type 2 diabetes mellitus: current and emerging agents. Drugs 2011;71:1675–88.
[13] Greig NH, Tweedie D, Rachmany L, Li Y, Rubovitch V, Schreiber S, et al. Incretin mimetics as pharmacologic tools to elucidate and as a new drug strategy to treat traumatic brain injury. Alzheimers Dement 2014;10:S62–75.
[14] Marzioni M, Alpini G, Saccomanno S, Candelaresi C, Venter J, Rychlicki C, et al. Glucagon-like peptide-1 and its receptor agonist exendin-4 modulate cholangiocyte adaptive response to cholestasis. Gastroenterology 2007;133:244–55.
[15] Wild D, Wicki A, Mansi R, Behe M, Keil B, Bernhardt P, et al. Exendin-4-based radiopharmaceuticals for glucagonlike peptide-1 receptor PET/CT and SPECT/CT. J Nucl Med 2010;51:1059–67.
[16] Psimadas D, Fani M, Zikos C, Xanthopoulos S, Archimandritis SC, Varvarigou AD. Study of the labeling of two novel RGD-peptidic derivatives with the precursor $[^{99m}Tc(H_2O)(CO)^3]^+$ and evaluation for early angiogenesis detection in cancer. Appl Radiat Isot 2006;64:151–9.
[17] Garcia MF, Zhang X, Gallazzi F, Fernandez M, Moreno M, Gambini JP, et al. Evaluation of tricine and EDDA as co-ligands for 99mTc-labeled HYNIC-MSH analogs for melanoma imaging. Anticancer Agents Med Chem 2015;15:122–30.
[18] Decristoforo D, Faintuch BL, Rey A, von Guggenberg E, Rupprich M, Hernandez-Gonzales I, et al. [^{99m}Tc]HYNIC-RGD for imaging integrin $\alpha_v\beta_3$ expression. Nucl Med Biol 2006;33:945–52.
[19] Faintuch BL, Santos RLSR, Souza ALFM, Hoffman TJ, Greeley M, Smith CJ. ^{99m}Tc-HYNIC-bombesin (7–14)NH_2: radiochemical evaluation with co-ligands EDDA (EDDA=Ethylenediamine-N,N'-Diacetic acid), tricine, and nicotinic acid. Synth React Inorg Met Org Chem 2005;35:43–51.
[20] Faintuch BL, Oliveira EA, Nunez EGF, Moro AM, Nanda PK, Smith CJ. Comparison of two peptide radiotracers for prostate carcinoma targeting. Clinics 2012;67:163–70.
[21] Faulks SC, Turner N, Else PL, Hulbert AJ. Calorie restriction in mice: effects on body composition, daily activity, metabolic rate, mitochondrial reactive oxygen species production, and membrane fatty acid composition. J Gerontol A Biol Sci Med Sci 2006;61:781–94.
[22] Milburn Jr JL, Hirose H, Lee YH, Nagasawa Y, Ogawa A, Ohneda M, et al. Pancreatic beta-cells in obesity. Evidence for induction of functional, morphologic, and metabolic abnormalities by increased long chain fatty acids. J Biol Chem 1995;270:1295–9.

[23] Marrif HI, Al-Sunousi SI. Pancreatic β cell mass death. Front Pharmacol 2016;7:1–16.
[24] Laurent D, Vinet L, Lamprianou S, Daval M, Filhoulaud G, Ktorza A, et al. Pancreatic β-cell imaging in humans: fiction or option? Diabetes Obes Metab 2016;18:6–15.
[25] Runge S, Schimmer S, Oschmann J, Schiødt CB, Knudsen SM, Jeppesen CB, et al. Differential structural properties of GLP-1 and exendin-4 determine their relative affinity for the GLP-1 receptor N-terminal extracellular domain. Biochem 2007;46: 5830–40.
[26] Mann RJ, Nasr NE, Sinfield JK, Paci E, Donnelly D. The major determinant of exendin-4/glucagon-like peptide 1 differential affinity at the rat glucagon-like peptide 1 receptor N-terminal domain is a hydrogen bond from SER-32 of exendin-4. Br J Pharmacol 2010;160:1973–84.
[27] Butler AE, Janson J, Bonner-Weir S, Ritzel R, Rizza RA, Butler PC. Beta-cell deficit and increased beta-cell apoptosis in humans with type 2 diabetes. Diabetes 2003;52: 102–10.
[28] Madsbad S. The role of glucagon-like peptide-1 impairment in obesity and potential therapeutic implications. Diabetes Obes Metab 2014;16:9–21.
[29] Wajchenberg BL. Postprandial glycemia and cardiovascular disease in diabetes mellitus. Arq Bras Endocrinol Metabol 2007;51:212–21.
[30] Gupta NA, Mells J, Dunham RM, Grakoui A, Handy J, Saxena NK, et al. Glucagon-like peptide-1 receptor is present on human hepatocytes and has a direct role in decreasing hepatic steatosis *in vitro* by modulating elements of the insulin signaling pathway. J Hepatol 2010;51:1584–92.
[31] Graaf CD, Donnelly D, Wootten D, Lau J, Sexton PM, Miller LJ, et al. Glucagon-like peptide-1 and its class B G protein-coupled receptors: a long march to therapeutic successes. Pharmacol Rev 2016;68:954–1013.
[32] Kahles F, Meyer C, Möllmann J, Diebold S, Findeisen HM, Lebherz C, et al. GLP-1 secretion is increased by inflammatory stimuli in an IL-6-dependent manner, leading to hyperinsulinemia and blood glucose lowering. Diabetes 2014; 63:3221–9.
[33] Carbone LJ, Angus PW, Yeomans ND. Incretin-based therapies for the treatment of non-alcoholic fatty liver disease: a systematic review and meta-analysis. J Gastroenterol Hepatol 2016;31:23–31.
[34] Dong Y, Lv Q, Li S, Wu Y, Li L, Li J, et al. Efficacy and safety of glucagon-like peptide-1 receptor agonists in non-alcoholic fatty liver disease: a systematic review and meta-analysis. Clin Res Hepatol Gastroenterol 2017 [pii: S2210–7401].
[35] Peyot ML, Pepin E, Lamontagne J, Latour MG, Zarrouki B, Lussier R, et al. Beta-cell failure in diet-induced obese mice stratified according to body weight gain: secretory dysfunction and altered islet lipid metabolism without steatosis or reduced beta-cell mass. Diabetes 2010;59:2178–87.
[36] Rydén A, Nyman G, Nalin L, Andreasson S, Korsgren O, Eriksson O, et al. Cardiovascular side-effects and insulin secretion after intravenous administration of radiolabeled Exendin-4 in pigs. Nucl Med Biol 2016;43:397–402.
[37] Selvaraju RK, Thomas N, Bulenga TN, Espes D, Lubberink M, Sörensen J, et al. Dosimetry of [68Ga]Ga-DO3A-VS-Cys40-Exendin-4 in rodents, pigs, non-human primates and human - repeated scanning in human is possible. Am J Nucl Med Mol Imaging 2015;5:259–69.
[38] Ingle D. A simple means of producing obesity in the rat. Proc Soc Exp Biol Med 1949; 72:604–5.
[39] Hariri N, Thibault L. High-fat diet-induced obesity in animal models. Nutr Res Rev 2010;23:270–99.